Fuel 303 (2021) 121269

Contents lists available at ScienceDirect

Fuel

journal homepage: www.elsevier.com/locate/fuel

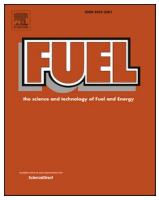

Full Length Article

Hydrogen-rich syngas production from chemical looping gasification of lignite by using $NiFe_2O_4$ and $CuFe_2O_4$ as oxygen carriers

Kun Zhao [a,b,c], Xiaojie Fang [d], Zhen Huang [a,b,c], Guoqiang Wei [a,b,c], Anqing Zheng [a,b,c,*], Zengli Zhao [a,b,c]

[a] Guangzhou Institute of Energy Conversion, Chinese Academy of Sciences, Guangzhou 510640, PR China
[b] CAS Key Laboratory of Renewable Energy, Guangzhou 510640, PR China
[c] Guangdong Provincial Key Laboratory of New and Renewable Energy Research and Development, Guangzhou 510640, PR China
[d] School of Chemical Engineering, Nanjing University of Science & Technology, Nanjing 210094, PR China

ARTICLE INFO

Keywords:
Coal gasification
Chemical looping gasification
H_2-rich syngas
Copper ferrite
Nickel ferrite

ABSTRACT

Chemical looping gasification provides a novel technology to enable clean conversion of coal with inherent CO_2 capture. In this study, four types of $NiFe_2O_4$ and $CuFe_2O_4$ synthesized by sol–gel method and solid-phase method were used as oxygen carriers to promote the H_2 production from gasification of lignite. The effects of the types of oxygen carrier and oxygen carrier to coal (O/C) ratio on chemical looping gasification of lignite were first investigated by a thermogravimetric analyzer (TGA) combing with various analytical methods. The results show that, among four types of oxygen carrier, the $NiFe_2O_4$ synthesized by sol–gel method exhibits the highest gasification reactivity with lignite char at an O/C ratio of 1, since its highly cubic spinel structure is beneficial to improve the mobility of lattice oxygen. Furthermore, the operating conditions for chemical looping gasification of lignite were optimized and the gasification performance of four types oxygen carriers was compared by using a fixed bed reactor. It is found that $NiFe_2O_4$ synthesized by sol–gel method exhibits the highest total gas yield of 24.47 mol/kg and H_2/CO ratio of 0.77 during chemical looping gasification of lignite under the optimal operating conditions, ascribed to Fe-Ni synergistic effect which provided higher gasification reactivity with lignite char. The addition of steam drastically improves the total gas yield and H_2/CO ratio of syngas from 24.47 mol/kg and 0.77 to 64.98 mol/kg and 2.79, suggesting that the H_2/CO ratio of syngas can be flexibly adjusted to meet the need of downstream process via controlling the amount of steam added. These findings provide an efficient method to obtain H_2-rich syngas via chemical looping gasification of lignite.

1. Introduction

With the steady population growth and economic development, the global energy consumption has increased gradually and is expected to continue to increase, especially in major emerging countries. The global primary energy consumption grew by 1.3% in 2019, while the primary energy consumption of China increased by 4.4%. China accounted for 24.3% of global energy consumption and 77.3% of global growth [1]. Coal has dominated the energy consumption of China over the last half century. The total coal consumption of China in 2019 was about 2.804 billion tons of standard coal equivalent (SCE), accounting for about 57.7% of the total energy consumption. It can be foreseen that coal will still dominate China's energy consumption in the next few decades. However, the conventional coal-fired power plants in China usually provides high air pollutant and greenhouse gas emissions. As the world's largest emitter of CO_2, China has pledged to reach peak carbon dioxide emissions before 2030 and carbon neutrality before 2060. The Chinese government has issued stringent environmental regulation and policy initiatives in order to drive the development of clean coal technologies to replace existing coal-fired power plants.

Gasification is a promising technology that offers a clean and efficient way to convert solid coal into syngas. Syngas from coal-gasification, primarily consisting of H_2 and CO, has been employed as a versatile platform for generating various desired products, such as electric power, heat, hydrogen, methane, methanol, dimethyl ether, Fischer-Tropsch (FT) liquids, and ammonia [2–4]. During gasification, coal is partially oxidized by gasifying agent at high temperature to form syngas via a series of oxidization and reforming reactions [5]. Typical

* Corresponding author at: Guangzhou Institute of Energy Conversion, Chinese Academy of Sciences, Guangzhou 510640, PR China.
E-mail address: zhengaq@ms.giec.ac.cn (A. Zheng).

https://doi.org/10.1016/j.fuel.2021.121269
Received 23 April 2021; Received in revised form 3 June 2021; Accepted 13 June 2021
Available online 18 June 2021

gasifying agents used are substoichiometric oxygen, air, steam, CO_2, or their mixtures. The desired oxygen in coal gasification is typically 20 to 40 percent of the stoichiometric oxygen required for complete oxidation. The heat released by partial oxidation of coal provides the energy required to drive the endothermic reactions during coal gasification. However, conventional air gasification results in a low-quality syngas with low calorific value (4–8 MJ/Nm^3) due to the dilution effect of nitrogen in the air. Pure oxygen or oxygen-enriched air gasification typically require a cryogenic air separation unit, resulting in higher investment/operation costs and a sharp reduction in energy efficiency. Hence, a novel gasification process, namely coal chemical looping gasification (CCLG), has been developed for producing high-quality syngas from coal [6–8]. CCLG utilizes lattice oxygen within oxygen carrier instead of molecular oxygen as gasifying agent [9,10]. During CCLG, coal is first pyrolyzed into volatiles and char, which are partially oxidized by the oxygen carrier to produce syngas in the fuel reactor. The reduced oxygen carrier is subsequently transferred from the fuel reactor to the air reactor where it is regenerated by air oxidization [11–13]. The oxygen and heat required to drive endothermic gasification reactions in the fuel reactor is supplied by circulating hot oxygen carrier regenerated from exothermic oxidization in the air reactor. This CCLG process, preventing the direct contact between coal and air, can avoid the need for cryogenic air separation unit to achieve a non-nitrogen diluted syngas, thereby eliminating the energy and cost penalty associated with CO_2 capture [14–16].

H_2 has been considered as a unique zero-emission energy carrier in future energy systems. It is generally accepted that the high H_2/CO ratio of syngas is beneficial for its subsequent separation, combustion, or catalytic synthesis units [17]. Depending on the purpose of the downstream process, the composition of syngas needs to be adjusted preferentially. The composition of syngas is highly dependent upon the nature of oxygen carrier and operating conditions of CCLG. Design and development of suitable oxygen carrier and optimization of operating conditions for CCLG is the key to produce hydrogen-rich syngas. The common oxygen carrier used for CCLG consists of naturally occurring ores and transition metal oxides, such as natural iron ores, Co, Mn, Ni, Fe, and Cu oxides [18–20]. The favorable properties of oxygen carrier include low cost, high oxygen storage and transport capacity, high reactivity in redox reactions, high mechanical and thermal stability. Among these oxygen carriers, Fe-based oxygen carrier appears to be an attractive candidate due to its low cost, abundant natural source, high oxygen transport capacity and environmental friendliness [21]. Wei and co-workers demonstrated that chemical looping gasification of lignite with hematite as oxygen carrier is capable of obtaining high quality syngas. It is found that the crystal phase evolution of hematite oxygen carrier during chemical looping gasification follows the reaction path of $Fe_2O_3 \rightarrow Fe_{0.963}O \rightarrow Fe_2O_3$ [22]. However, Fe-based oxygen carrier exhibited low redox reaction rate with coal, especially coal char. The solid–solid reaction between char and oxygen carrier is the rate-limiting step during CCLG. Ni and Cu-based oxygen carriers exhibits very high reactivity with coal. Shen and co-workers found that NiO exhibited high reactivity above 900 °C during chemical looping combustion of coal, and the CO_2 concentration (dry basis) in the exit gas of the fuel reactor was nearly 95% [23]. Dennis and co-workers showed that the gasification rates of lignite and its derived char over CuO/γ-Al_2O_3 at 900 °C were significant, and CuO/γ-Al_2O_3 acted as a durable oxygen carrier over 20 redox cycles. It was observed that CuO decomposed at 900 °C to generate O_2 and Cu_2O, and both reacted with CO produced by gasification, whilst the O_2 reacted directly with the lignite derived char[24]. Unfortunately, Ni and Cu are expensive, toxic and, carcinogenic [25,26]. As a novel kind of mixed metal oxide, ferrites (MFe_2O_4) with a spinel structure have attracted increasing attention due to its high thermal stability, good magnetic properties and high oxygen capacity [27]. Among various ferrites, $NiFe_2O_4$ and $CuFe_2O_4$ are the most potential ones since Fe-based oxygen carrier cooperated with highly reactive Ni and Cu can combine the complementary advantages of individual Fe or Ni/Cu. Ignacio J. et al. used NiFe2O4 as catalyst for the chemical looping conversion of CO_2 and found that Ni-Fe clusters forming on the surface of the ferrite nanoparticle result from the segregation of metal atoms recruited from octahedral sites of the Ni-ferrite. Such change in the chemistry and structure of the catalyst has a profound impact on the activity of the catalyst [28]. Huang et al. confirmed the good reactivity of $NiFe_2O_4$ in the biomass chemical looping gasification process [29]. Marcel et al. tested $NiFe_2O_4$ as a combined catalyst precursor and oxygen transfer material for improved conversion of methane into syngas [30]. The superior behavior of nickel iron oxide compared to iron oxide were demonstrated and the enhanced catalytic activity is attributed to the generation of fresh nickel surfaces during the reduction of the metal oxide. Niu et al. evaluated the combustion performance in chemical looping combustion of sewage sludge in a batch fluidized-bed reactor by using $CuFe_2O_4$ as oxygen carrier. The formation of $CuFe_2O_4$ could improve both the reactivity of Fe_2O_3 species through synergetic effect and the physical stability of CuO during redox reactions [31]. Zhu et al. investigated $CuFe_2O_4$ as oxygen carrier for coal chemical looping gasification and found that presence of ferrite better relieved the deep oxygen loss of $CuFe_2O_4$. Synergistic effect between Cu-Fe made a great contribution to the reduction process [32].

Up to data, there is a lack of information on the comparative assessment of chemical looping gasification of coal over different $NiFe_2O_4$ and $CuFe_2O_4$ oxygen carriers to produce H_2-rich syngas. Herein, four types of $NiFe_2O_4$ and $CuFe_2O_4$ are synthesized by sol–gel method and solid-phase method. Several researchers have observed that different synthesis methods can influence the size and morphology of ferrites nanoparticles and hence affect the activity [33]. As generally known, sol–gel method is the most effective method for the preparation of ferrites due to its advantages such as high homogeneity, good dispersibility, and easy operability. Meanwhile, solid-phase method was also commonly chosen because it's more suitable for the oxygen carrier synthesis in large quantity. These two routes are expected to introduce morphological variation and different degree of interaction between the metals, which can modulate the catalytic performance. Chemical looping gasification of lignite over $NiFe_2O_4$ and $CuFe_2O_4$ is proposed for achieving efficient gasification of lignite. The effect of preparation methods of $NiFe_2O_4$ and $CuFe_2O_4$ and operating conditions (e.g., oxygen carrier to coal ratio, gasification temperature, reaction time, carrier gas flowrate, and the addition of steam) on the chemical looping gasification of lignite is systematically investigated by using thermogravimetric analyzer (TGA) and a fixed bed reactor. The oxygen carriers are characterized by XRD, H_2-TPR, and SEM. After the comparative assessment of oxygen carriers and the optimization of operating conditions, the technical feasibility to produce H_2-rich syngas from chemical looping of lignite over selected oxygen carrier is thus verified and discussed.

2. Experimental section

2.1. Materials and preparation

The coal sample used in the experiment is Yunnan lignite. The raw lignite was crushed by a pulverizer and sieved to obtain a coal sample with a particle size of 80–100 mesh. The lignite was dried at 105 °C for 48 h, and stored in a dryer for later use after moisture removal. The proximate, ultimate analysis and heating value of lignite are shown in Table 1. The proximate analysis of lignite was tested based on the national standard GB/T212-2008. The elemental analysis of lignite was carried out on an elemental analyzer (Vario EL, Elementar). The higher heating value (HHV) of lignite was analyzed by using a bomb calorimeter (WZR-1 T-CII, Bente).

$CuFe_2O_4$ (or $NiFe_2O_4$) was prepared by sol–gel method and solid-phase method. For the sol–gel method: the desired amounts of Fe $(NO_3)_3{\cdot}9H_2O$ (Aladdin, AR 99.99%), $Cu(NO_3)_2{\cdot}3H_2O$ (Aladdin, AR 99.99%), $Ni(NO_3)_2{\cdot}6H_2O$ (Aladdin, AR 98%) and citric acid (Macklin, AR 99.5%) were dissolved in deionized water under constant stirring for

Table 1
The proximate, ultimate analysis and heating value of lignite.

Proximate analysis (wt.%, ad)				Ultimate analysis (wt.%, db)					Higher heating value (KJ/Kg)
V	FC	M	A	C	H	N	S	O[a]	21428.65
43.44	33.23	6.86	16.47	51.73	4.27	1.24	1.12	41.64	

ad: Air dried, db: Dry basis.

1 h at room temperature. The molar ratio of Fe to Cu (or Ni) to citric acid was 2:1:3.9. The aqueous solution was heated in a water bath (80 °C) under constant stirring to form gel. The resulting gel was dried at 105 °C for 24 h. The dried precursor was calcinated in a muffle furnace at 400 °C with a heating rate of 10 °C/min for 2 h, and then heated to 900 °C with a heating rate of 10 °C/min and held there for 6 h. The resulting sample was ground to obtain fresh oxygen carrier around 100 mesh. For the solid-phase method: the desired amounts of iron oxide (Macklin, AR 99.95%) and copper oxide (Macklin, AR 99%) or nickel oxide (Aladdin, AR 99%) were ground and mixed evenly in a mortar. The molar ratio of Fe to Cu (or Ni) was 2:1. The mixture was calcinated at 900° C for 6 h to obtain fresh oxygen carrier. Finally, the obtained oxygen carriers were granulated and screened to 100 mesh.

2.2. Characterization of oxygen carrier

The crystalline phases of oxygen carriers were analyzed by an X-ray powder diffractometer (XRD) (X'Pert Pro MPD, PANalytical B.V.) with Cu Kα radiation (k = 1.54060 Å) at 40 kV and 40 mA in the scanning range of 2θ = 5-80° with a step size of 0.0167°. The morphology of oxygen carrier was recorded by using a scanning electron microscope (SEM) (S-4800, Hitachi). The hydrogen temperature programmed reduction (H_2-TPR) of oxygen carrier was carried out in a full-automatic temperature programmed chemisorption analyzer (CPB-1, Quantachrome). The oxygen carrier was firstly heated to 300 °C with a heating rate of 20 °C /min under helium atmosphere to remove air from the system, and then cooled to 40 °C. After that, the gas atmosphere was switched to 10% H_2/Ar. The sample was subsequently heated to 900 °C with a heating rate of 20 °C/min. the surface morphology of oxygen carrier was characterized by the scanning electron microscopy (SEM) (Hitachi S-4800, Hitachi).

2.3. Chemical looping gasification of lignite in a TGA and a fixed bed reactor

The thermogravimetric and derivative thermogravimetric (TG/DTG) analysis for chemical looping gasification of lignite over $NiFe_2O_4$ and $CuFe_2O_4$ was carried out in a thermogravimetric analyzer (TGA) (PT1600, Netzsch, Germany). The lignite and oxygen carrier were mixed evenly with a desired mass ratio in a mortar. The mixtures were heated from 30 to 1100 °C with a heating rate of 10 °C/min. High-purity argon was used as carrier gas with a flow rate of 100 ml/min. The syngas production from chemical looping gasification of lignite was performed in a fixed-bed reactor. Lignite and oxygen carrier were mixed evenly with a desired mass ratio in a mortar. The mixtures were fed into the fixed bed reactor via a ball valve. The chemical looping gasification of lignite was conducted at varying temperature (800–1000 °C) with a constant residence time of 1 h. High purity argon with a flow rate of 100 ml/min (unless otherwise stated) was used as the carrier gas. The syngas was collected by an airbag and then analyzed by a gas chromatography equipped with a thermal conductivity detector and a flame ionization detector (GC-TCD/FID). The formulas of gas composition, total gas yield, syngas selectivity, and carbon conversion are shown as follows. The gas composition (f_i) is defined as the molar fraction of individual gas (n_i) to the total molar fraction of all gaseous products (H_2, CO, CH_4, CO_2, and C_2H_m, except inert gas) (n), the molar fraction of individual gas was obtained from GC analysis:

$$f_i(\%) = \frac{n_i}{n} \times 100\%,\ i = H_2,\ CO,\ CH_4,\ C_2H_m,\ \text{and}\ CO_2,\ (m = 2,4\ \text{and}\ 6)$$

The total gas volume (V, L) is calculated according to the Ar balance between the inlet and outlet gas of chemical looping gasification of lignite. The total gas yield (Y_t) is defined as the total molar of all gaseous products (M) to the mass of lignite (m). The gas production of specific gas (Y_i, $i = H_2$, CO, CH_4, and CO_2) is defined as the molar of specific gaseous product (M_i, $i = H_2$, CO, CH_4, and CO_2) to the mass of lignite (m). The syngas selectivity (S) is defined as the total molar of H_2 and CO (V_f) to the total molar of all gaseous products (M):

$$Y_t(mol/kg) = \frac{V}{22.4 \times m} \times 100\%,\ Y_i(mol/kg) = f_i \times \frac{V}{22.4 \times m} \times 100\%,\ S = \frac{V_f}{M} \times 100\%$$

The carbon conversion (E) is defined as the percentage of the carbon converted into all carbon-containing gaseous products (CO, CH_4, CO_2, and C_2H_m) to the carbon in the lignite: $E(\%) = \frac{12 \times (f_{CO_2} + f_{CO} + f_{CH_4} + 2f_{C_2Hm}) \times Y_t}{22.4 \times C\%} \times 100\%$, where $C\%$ is the mass content of carbon in the lignite.

3. Results and discussion

3.1. The characterization of $NiFe_2O_4$ and $CuFe_2O_4$ synthesized by different methods

The $CuFe_2O_4$ and $NiFe_2O_4$ oxygen carriers were prepared by sol–gel method and solid-phase method. The prepared oxygen carriers were subsequently characterized by XRD. The XRD patterns of the oxygen carriers are shown in Fig. 1. It is evident that the two $CuFe_2O_4$ oxygen carriers have very similar XRD patterns. The diffraction peaks at 2θ = 18.3°, 29.9°, 35.3°, 35.9°, 43.9°, 58.0°, 62.1°, and 64.0° are respectively assigned to the reflections from the (101), (112), (103), (211), (220), (321), (224) and (400) crystal planes of $CuFe_2O_4$ (JCPDS No. 006–0545). Besides, unobvious crystalline planes of CuO and Fe_3O_4 can be observed for the $CuFe_2O_4$ synthesized by sol–gel method, indicating its relatively single-phase cubic spinel structure. But the peak intensity of CuO increase obviously for the $CuFe_2O_4$ synthesized by solid-phase method. The $NiFe_2O_4$ oxygen carrier prepared by sol–gel method also exhibits a single-phase cubic spinel structure. The diffraction peaks at 2θ = 30.3, 35.7, 37.3, 43.4, 53.8, 57.4 and 63.0° are attributed to the reflections from the (220), (311), (222), (400), (422), (511), (440) crystal planes of $NiFe_2O_4$ (JCPDS No. 054–0964). However, some extra diffraction peaks corresponding to the crystalline planes of α-Fe_2O_3 and NiO were found in the XRD pattern of the $NiFe_2O_4$ oxygen carrier prepared by solid-phase method, indicating that the $NiFe_2O_4$ oxygen carrier prepared by solid-stage method is a mixed phase of $NiFe_2O_4$, α-Fe_2O_3 and NiO.

The H_2-TPR profiles of $CuFe_2O_4$ and $NiFe_2O_4$ oxygen carriers synthesized by different methods are illustrated in Fig. 2. It is obvious that there are two well-defined peaks in the H_2-TPR profiles of $CuFe_2O_4$ oxygen carriers synthesized by sol–gel method and solid-phase method. The first reduction peak centered at 300–350 °C is attributed to the reduction of $CuFe_2O_4$ to Cu and Fe_2O_3. And the second reduction peak centered at 550–600 °C is ascribed to the reduction of Fe_2O_3 to Fe. However, the peak temperature of $CuFe_2O_4$ synthesized by sol–gel method is evidently lower than that of $CuFe_2O_4$ synthesized by solid-phase method, indicating that $CuFe_2O_4$ synthesized sol–gel method exhibit better reducibility at low temperature. Since the nitrate can be mixed more uniformly during the sol–gel synthetic process which may benefit the metal synergistic effect and enhance the reducibility. The

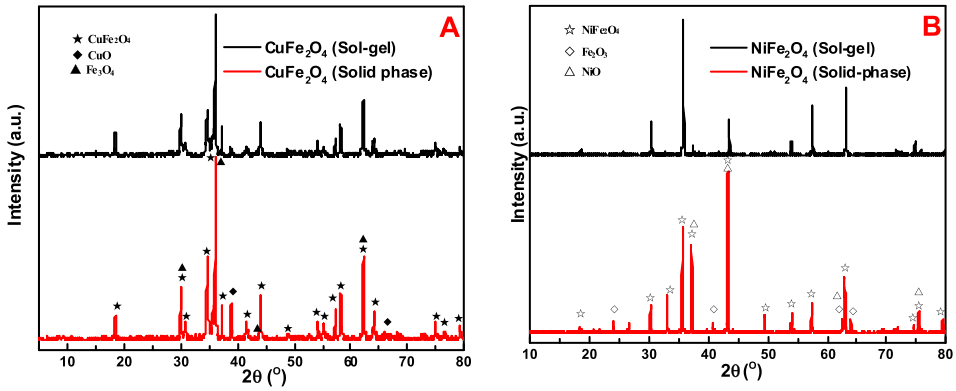

Fig. 1. The XRD pattern of synthesized $CuFe_2O_4$ and $NiFe_2O_4$ oxygen carriers. A: $CuFe_2O_4$ oxygen carriers, B: $NiFe_2O_4$ oxygen carriers.

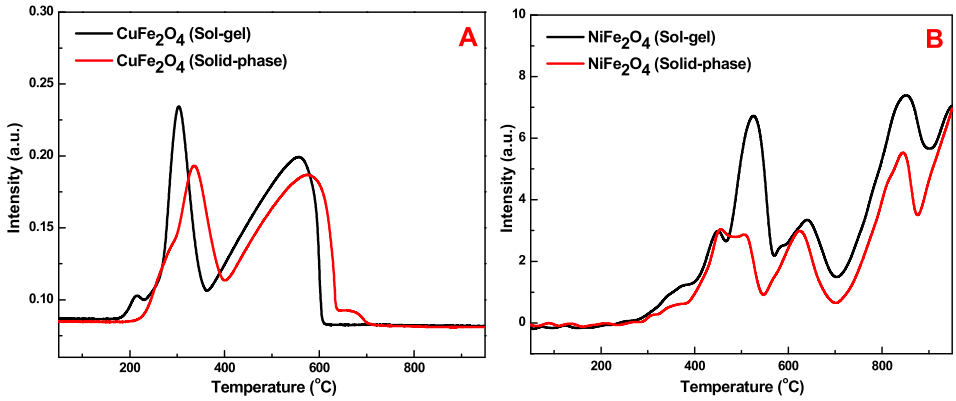

Fig. 2. The H_2-TPR profiles of synthesized $CuFe_2O_4$ and $NiFe_2O_4$ oxygen carriers. A: $CuFe_2O_4$ oxygen carriers, B: $NiFe_2O_4$ oxygen carriers.

reduction of $NiFe_2O_4$ is more complex than that of $CuFe_2O_4$ and a multi-step reduction pathway can be observed. The possible reduction pathway is shown as follows: $NiFe_2O_4$ → Ni and Fe_2O_3 → Ni and Fe_3O_4 → Ni and FeO → Ni and Fe. $NiFe_2O_4$ is first reduced to Ni and Fe_2O_3 at low temperatures (400–580 °C), and then Fe_3O_4 is generated at 580–700 °C via the partial reduction of Fe^{3+} to Fe^{2+}. The reduction of Fe_3O_4 to FeO occurs at high temperature (700–900 °C) due to that the elevating temperature favors this endothermic reaction. At last, Fe is formed via the reduction of FeO when the reaction temperature is greater than 875 °C. It is evident that the $NiFe_2O_4$ synthesized by sol–gel method provides higher area of reduction peak than that synthesized by solid-phase method, indicating that the highly cubic spinel structure of the $NiFe_2O_4$ synthesized by sol–gel method is beneficial to improve the mobility of lattice oxygen. It is worthy to note that the reduction temperature of $CuFe_2O_4$ is obviously lower than that of $NiFe_2O_4$. The result may be due to the hydrogen spillover from Cu to Fe_2O_3 caused by the strong interaction between Cu and Fe_2O_3 [34]. It is well accepted that $CuFe_2O_4$ is easily reduced to Cu and Fe_2O_3 at low temperatures. H_2 is first adsorbed and dissociated by Cu on the catalyst's surface to form atomic hydrogen, which are subsequently migrated from Cu metal surface to Fe_2O_3, thus achieving the reduction of Fe_2O_3 at a lower temperature due to the stronger reducibility of atomic hydrogen.

3.2. *The reactivity analysis for chemical looping gasification of lignite with different oxygen carriers by using TGA*

The reactivity of $CuFe_2O_4$ and $NiFe_2O_4$ oxygen carriers during chemical looping gasification of lignite was investigated by using TGA.

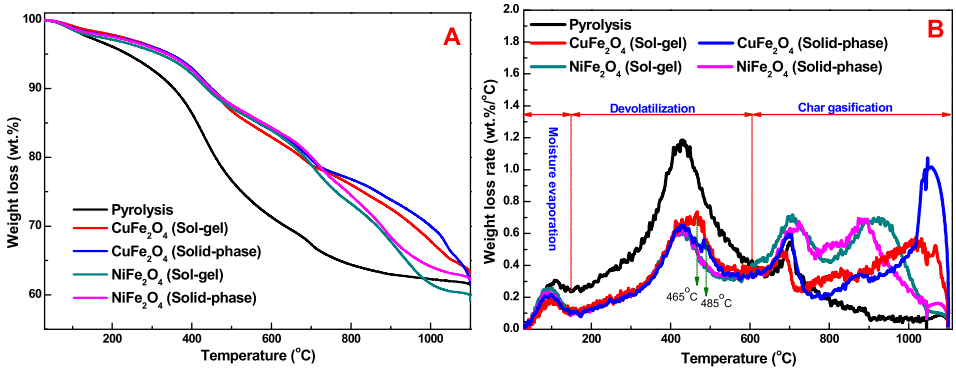

Fig. 3. The weight loss (TG) and weight loss rate (DTG) curves for chemical looping gasification of lignite over $CuFe_2O_4$ and $NiFe_2O_4$ synthesized by different methods. The oxygen carrier to coal ratio is 1:1. Pyrolysis: pyrolysis of lignite without oxygen carrier. A: TG curves, B: DTG curves.

The weight loss (TG) and weight loss rate (DTG) curves for chemical looping gasification of lignite over different oxygen carriers are showed in Fig. 3A and B. The occurrence of lignite gasification can be confirmed and the reactivity was significantly affected by the type of oxygen carrier. As shown in the Fig. 3B, the DTG curves for pyrolysis or chemical looping gasification of lignite can be divided into three stage. The first weight loss stage between 30 and 150 °C is attributed to the moisture evaporation. The second weight loss stage between 150 and 600 °C is mainly associated with the devolatilization reactions of lignite. It can be seen that the weight loss of lignite pyrolysis is overwhelmingly happened during the first devolatilization stage, indicating that all the lignite without oxygen carrier is pyrolysis to release the volatiles. It should be noted that a shoulder peak centered at about 465 or 485 °C is observed during chemical looping gasification of lignite with the two types of $CuFe_2O_4$ oxygen carriers, which could be ascribed to the reforming of $CuFe_2O_4$ with the volatiles from lignite pyrolysis. This result is corresponded with the H_2-TPR results presented in Fig. 2A. Besides, it is also found that the $CuFe_2O_4$ oxygen carrier synthesized by sol–gel method exhibits higher maximum weight loss rate at this temperature, indicating that it has higher reforming reactivity with the pyrolysis volatiles. The last weight loss stage between 600 and 1100 °C is primarily ascribed to the lignite char gasification with oxygen carrier. The only DTG peak centered at approximately 700 °C during lignite pyrolysis without oxygen carrier is associated with the condensation reactions of lignite char, as well as the decomposition of mineral matter within ash (e.g., the decomposition of pyrite into pyrrhotite and/or iron sulfide) at this temperature [35]. While for the samples over $CuFe_2O_4$ and $NiFe_2O_4$ oxygen carriers, two well-defined DTG peaks are observed for chemical looping gasification of lignite char at this stage. These gasification peak intensities are significantly improved when comparing with the pyrolysis of lignite without oxygen carrier, indicating that the lignite char can be effectively gasified by adding oxygen carrier, and different oxygen carriers provide different gasification reactivity with lignite char. The DTG peak centered at 680–700 °C for $CuFe_2O_4$ oxygen carriers is predominantly attributed to the condensation of lignite char and the reduction of Fe_2O_3 with lignite char, due to its higher peak intensity than that of lignite pyrolysis. Furthermore, there is a DTG peak centered at 1030–1050 °C for $CuFe_2O_4$ oxygen carriers, which can be related to the gasification of char with O_2. It is speculated that CuO decomposes at high temperature to form Cu_2O and O_2 [36]. It is obvious that $CuFe_2O_4$ synthesized by sol–gel method provides higher reforming reactivity with pyrolysis volatiles and lower gasification reactivity with lignite char when comparing with $CuFe_2O_4$ synthesized by solid-phase method. That mainly because the Cu-Fe synergistic effect between $CuFe_2O_4$ oxygen carriers synthesized by solid method are weaker than that made by sol–gel method, and higher temperature benefits the decompose of CuO and leads to the char combustion at 1030–1050 °C. This result is also corresponded to the XRD results that showed higher CuO intensity peak for $CuFe_2O_4$ synthesized by solid method. The DTG peak centered at 700–720 °C for $NiFe_2O_4$ oxygen carriers is associated with the condensation of lignite and the gasification of char with $NiFe_2O_4$ to form syngas, Ni and Fe_2O_3. The DTG peak centered at 880–930 °C for $NiFe_2O_4$ oxygen carriers is ascribed to the char gasification with Fe_2O_3. The $NiFe_2O_4$ oxygen carrier synthesized by sol–gel method shows the highest weight loss rate in this last stage, indicating that it exerts the highest gasification reactivity with lignite char. The result could be due to the best mobility of lattice oxygen within $NiFe_2O_4$ oxygen carrier synthesized by sol–gel method, which is further confirmed by the result obtained from Fig. 2B. It is worth noting that these DTG peaks are not in line with the reduction peaks obtained from H_2-TPR. The results could be due to the difference in the reducibility of lignite char and H_2.

The TG/DTG curves for chemical looping gasification of lignite over $NiFe_2O_4$ oxygen carrier synthesized by sol–gel method with varying oxygen carrier to coal ratio (O/C ratio) are plotted in Fig. 4A and B. It is observed that the intensity of the peak centered at 430 °C, related to the devolatilization reactions of lignite at the second stage, decreases continuously with increasing O/C ratio. It is due to the decreasing content of lignite in the mixture of oxygen carriers and lignite. Elevating O/C ratio from 0 to 1 significantly improved the maximum weight loss rate for both two peaks in the stage of char gasification, suggesting that the increasing supply of lattice oxygen within $NiFe_2O_4$ is beneficial to improve the gasification reactivity of lignite char. However, further elevating O/C ratio from 1 to 3/1, their peak temperature shifts toward high temperature. The results might be attributed to that too high O/C ratio gives the less contact between lignite char and oxygen carrier. The optimal O/C ratio for chemical looping of lignite over $NiFe_2O_4$ oxygen carrier synthesized by sol–gel method is 1 according to the TG/DTG results.

3.3. *The optimization of operating conditions for chemical looping gasification of lignite over $NiFe_2O_4$ synthesized by sol–gel method.*

The $NiFe_2O_4$ synthesized by sol–gel method was selected as the oxygen carrier for the optimization of operating conditions of chemical looping gasification of lignite, since it can provide the highest gasification reactivity with lignite char. The effect of reaction temperature on the performance of chemical looping gasification of lignite is presented in Fig. 5. It can be seen that the gasification temperature exerts significant impact on the gas yield, carbon conversion and syngas selectivity. As the gasification temperature increases from 800 °C, the total gas yield, carbon conversion, and syngas selectivity first increased and then start to decrease when the gasification temperature went to 950 °C. The maximum values of total gas yield, carbon conversion, and syngas selectivity can reach 24.5 mol/kg, 40.43%, and 69.0% respectively at the gasification temperature of 900 °C. It is well accepted that elevating gasification temperature can significantly promote the gasification rate of oxygen carrier with pyrolysis volatiles and char, thus improving the

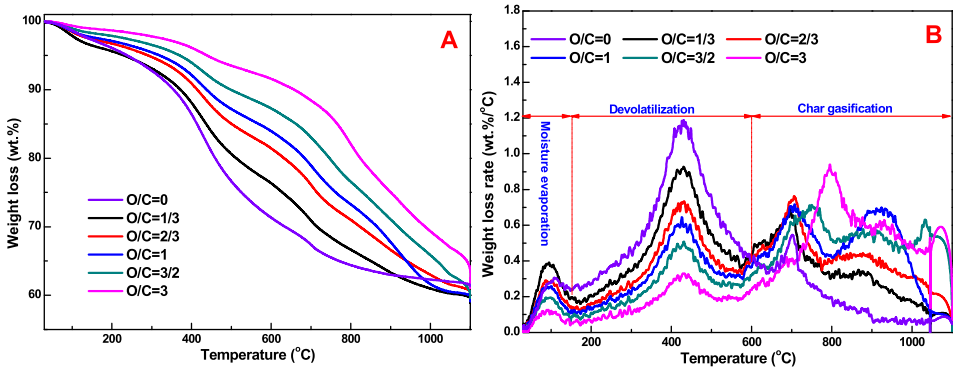

Fig. 4. The weight loss (TG) and weight loss rate (DTG) curves for chemical looping gasification of lignite over $NiFe_2O_4$ synthesized by sol–gel method with varying oxygen carrier to coal ratio. O/C ratio of 0 corresponds to pyrolysis of lignite without oxygen carrier. A: TG curves, B: DTG curves.

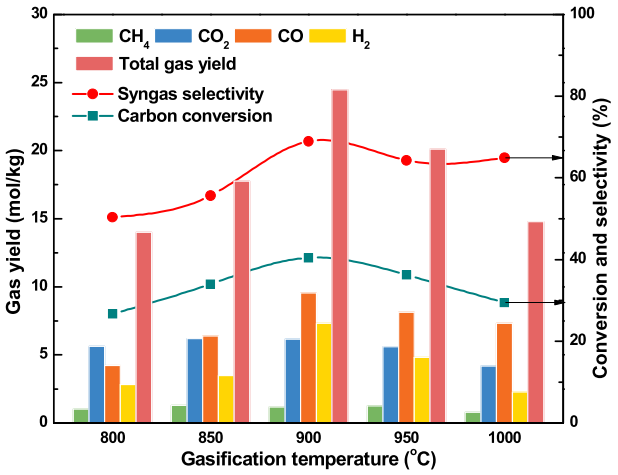

Fig. 5. The effect of gasification temperature on chemical looping gasification of lignite. Oxygen carrier: $NiFe_2O_4$ synthesized by sol–gel method, O/C ratio = 1, reaction time: 60 min, Ar flowrate: 100 ml/min.

carbon conversion and syngas production during chemical looping gasification of lignite. However, high-temperatures (950 °C) could cause the metal sintering and particle agglomeration of the $NiFe_2O_4$ oxygen carrier [37]. Both phenomena significantly reduce the gasification rate and performance of the $NiFe_2O_4$ oxygen carrier during lignite gasification. This challenge could be effectively overcome via applying highly dispersed $NiFe_2O_4$ on inert support (e.g., Al2O3, SiO_2, TiO2, and ZrO2) as oxygen carrier.

The evolution profiles of syngas production from chemical looping gasification of lignite as a function of reaction time is depicted in Fig. 6A. As the reaction time increases, the total gas yield first increases and then smoothly dropped. The maximum total gas yield of 7.34 mol/kg and the highest syngas yield of 4.53 mol/kg are reached during the reaction process from 5 to 10 min. The carbon conversion and syngas selectivity also firstly increase and reach their maximum values at the reaction time of 10 to 15 min. As the reaction time reaches 35 min, the syngas selectivity starts to increase considerably. When the reaction time is greater than 60 min, the total gas yield is very low (<0.1 mol/kg), implying that the gasification rate becomes very slow at that time. The results could be explained by two possible reasons. One is the deactivation of oxygen carrier at that time caused by the cracking of CO_2 on oxygen carrier to form coke. Another one is the complete release of volatiles from lignite at that time. The residual volatiles release from lignite char is the key for initiating the solid–solid reaction between oxygen carrier and lignite char [38]. It is thus concluded that the suitable reaction time for chemical looping gasification should be greater than 35 min to ensure the effective conversion of lignite char. The effect of Ar flowrate on the syngas production from chemical looping gasification of lignite is shown in Fig. 6B. It is evident that the optimal flowrate is 100 ml/min, since it provides the maximum the total gas yield, CO yield, H_2 yield, carbon conversion and syngas selectivity. The Ar flowrate is related with the vapor residence time. Low Ar flowrate, corresponding to long vapor residence time, may promotes the vapor reforming reactions, such as the reverse water–gas shift reaction, thus resulting in the low gas yield. In addition, low Ar flowrate may improves the cracking of CO_2 over partially reduced $NiFe_2O_4$ to form CO and coke. The serious coke of oxygen carrier causes the rapid deactivation of oxygen carrier, thus resulting in the low carbon conversion. Too high Ar flowrate, meaning too short residence time, causes the short contact time between $NiFe_2O_4$ and pyrolysis vapors, also leading to the low gas yield and carbon conversion. It is well accepted that the volatiles release from lignite char could significantly impact the solid–solid reaction between oxygen carrier and lignite char[38]. Minor volatiles could initiate the solid–solid reaction, and subsequent the CO_2, derived from combustion of volatiles, induces an in-situ CO_2 gasification of lignite char via Boudouard reaction, which may become a driving force for the continuous reduction of the oxygen carrier and thus to produce CO_2. It is inferred that the volatiles can be rapidly carried out by the high flowrate, thus lowering the solid–solid reaction rate between lignite char and oxygen carrier. It is thus concluded that the optimal gasification temperature, reaction time, and Ar flowrate for chemical looping gasification of lignite are 900 °C, 60 min, and 100 ml/min.

3.4. *The syngas production from chemical looping gasification of lignite over different oxygen carriers*

The effect of O/C ratio on the syngas production from chemical looping gasification of lignite over two types of $CuFe_2O_4$ oxygen carrier under the optimal operating conditions was conducted in a fixed bed reactor. The O/C ratio of 0 corresponds to pyrolysis of lignite. It can be seen from Fig. 7 that the carbon conversion and total gas yield from pyrolysis of lignite are 18.1% and 13.04 mol/kg, respectively. For the syngas production from $CuFe_2O_4$ oxygen carrier synthesized by sol–gel as illustrated in Fig. 7A, the carbon conversion increases progressively from 18.1 to 64.4%, while the total gas yield increases from 13.04 to 30.69 mol/kg as the O/C ratio increases from 0 to 3. However, the syngas selectivity drops with increasing O/C ratio. The highest and lowest syngas selectivity of 71.9 and 54.8% are respectively obtained at the O/C ratio of 0 and 3. During chemical looping gasification lignite, lignite is first pyrolyzed to volatiles and char under thermal action. The pyrolysis volatiles and char are subsequently reacted with lattice oxygen

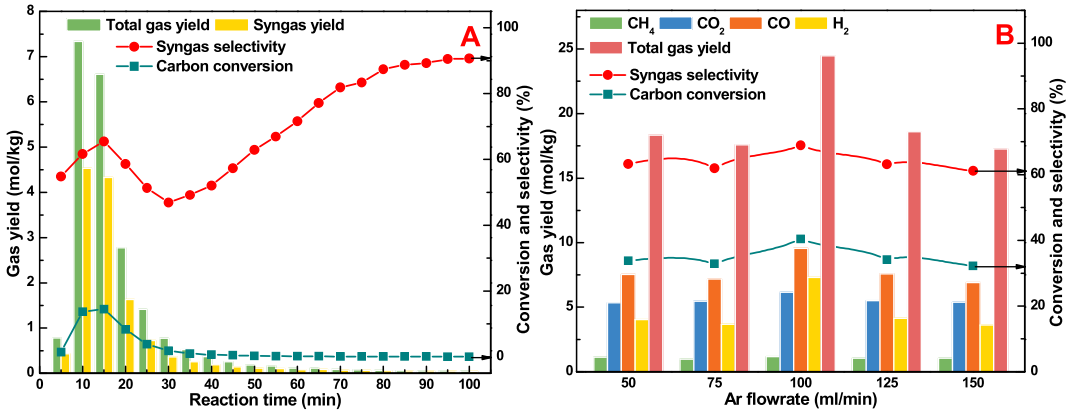

Fig. 6. The effects of reaction time and Ar flowrate on the syngas production from chemical looping gasification of lignite. Oxygen carrier: $NiFe_2O_4$ synthesized by sol–gel method, gasification temperature: 900 °C, O/C ratio = 1, reaction time: 60 min, except Fig. 8B, Ar flowrate: 100 ml/min, except Fig. 8A. A: Reaction time, B: Ar flowrate.

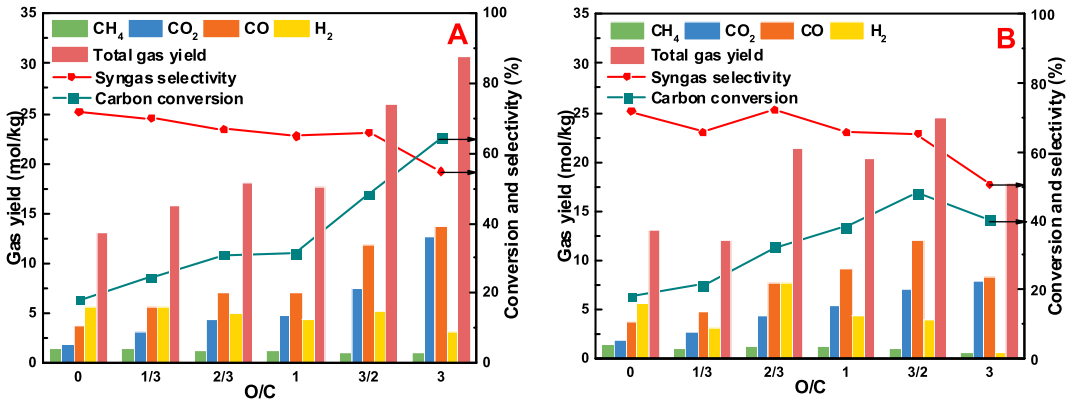

Fig. 7. The effect of oxygen carrier to coal ratio (O/C ratio) on chemical looping gasification of lignite over $CuFe_2O_4$ synthesized by different methods. O/C of 0 corresponds to pyrolysis of lignite without oxygen carrier. Gasification temperature: 900 °C, Reaction time: 60 min, Ar flowrate: 100 ml/min. A: $CuFe_2O_4$ synthesized by sol–gel method, B: $CuFe_2O_4$ synthesized by solid-phase method.

within the $CuFe_2O_4$ oxygen carrier to form CO, CO_2, H_2, CH_4, H_2O. The increasing O/C ratio provides more lattice oxygen, thus improving the conversion of volatiles and char into syngas and water. The speculation is verified by the fact that the CO_2 yield enhanced with increasing O/C ratio. The CO_2, CO, H_2 and CH_4 yields from lignite pyrolysis are 1.86, 3.76, 5.61, and 1.44 mol/kg. The CO and CO_2 yield are enhanced by adding the $CuFe_2O_4$ oxygen carrier synthesized by sol–gel method. As the O/C ratio increases from 0 to 3, the CO_2 yield increases continuously from 1.86 to 12.61 mol/kg, while the CO increases gradually from 3.76 to 13.65%. In contrast, the CH_4 and H_2 yield are reduced by adding the $CuFe_2O_4$ oxygen carrier. The increasing supply of lattice oxygen promotes the oxygenation of H_2, CO, CH_4, and char, resulting in the formation of more CO, CO_2, and H_2O.

The syngas production from $CuFe_2O_4$ oxygen carrier synthesized by solid-phase method is illustrated in Fig. 7B. Its highest total gas yield and carbon conversion of 24.4 mol/kg and 48.1% are obtained at the O/C ratio of 3/2. The maximum and minimum syngas selectivity of 72.2 and 50.6% are respectively generated at the O/C ratio of 2/3 and 3. The CO and CO_2 yield are enhanced by adding oxygen carrier, whereas the CH_4 and H_2 yield are reduced. As the O/C ratio increases from 1/3 to 3, the CO_2 yield increases from 2.70 to 7.99 mol/kg, while the CO and H_2 yield first increase and then decrease. The maximum CO yield of 11.94 mol/kg is obtained at the O/C ratio of 3/2. And the highest H_2 yield is produced at the O/C ratio of 2/3. It is evident that the gasification performance of this oxygen carrier is significantly different from that of the $CuFe_2O_4$ oxygen carrier synthesized by sol–gel method. It could be explained by the results obtained from Fig. 3B. The $CuFe_2O_4$ synthesized by solid-phase method gives lower reforming reactivity with pyrolysis volatiles and higher gasification reactivity with lignite char when comparing with $CuFe_2O_4$ synthesized by sol–gel method. It is thus concluded that, among the two types of oxygen carriers, the $CuFe_2O_4$ synthesized by solid-phase method is a better oxygen carrier, and its optimal O/C ratio is 2/3 for maximizing the H_2 yield.

The syngas production from chemical looping gasification of lignite over different $NiFe_2O_4$ oxygen carriers with varying O/C ratio is graphed in Fig. 8. Fig. 8A shows the gasification performance of $NiFe_2O_4$ synthesized by sol–gel method. The total gas yield and carbon conversion are enhanced by applying the $NiFe_2O_4$ oxygen carrier, whereas the syngas selectivity is reduced. The carbon conversion increases gradually from 18.1 to 61.2% with the O/C ratio increases from 0 to 3, while the total gas yield increases from 13.04 to 28.85 mol/kg. Simultaneously, the CO and CO_2 yield rise continuously as the increasing O/C ratio, whereas the CH_4 yield decreases gradually. As the O/C ratio increases from 1/3 to 3, the maximum syngas selectivity of 69.0% and the highest H_2 yield of 7.32 mol/kg are achieved at the O/C ratio of 1. The results are in accordance with those obtained from Fig. 4B. The optimal O/C ratio for chemical looping gasification of lignite over the $NiFe_2O_4$ synthesized by sol–gel method is 1 for maximizing the syngas selectivity. Fig. 8B provides the gasification performance of $NiFe_2O_4$ synthesized by solid-phase method. The carbon conversion, total gas yield, CO yield, and CO_2 yield rise gradually as the O/C ratio increases from 0 to 3, whereas the H_2 yield steadily decreases. Similar with the results reported for $CuFe_2O_4$ oxygen carriers, the increasing supply of lattice oxygen promotes the oxygenation of pyrolysis volatiles (e.g., H_2, CO and CH_4) and char, resulting in the formation of more CO, CO_2, and H_2O. The increase in the CO yield implies that the formation rate of CO is greater

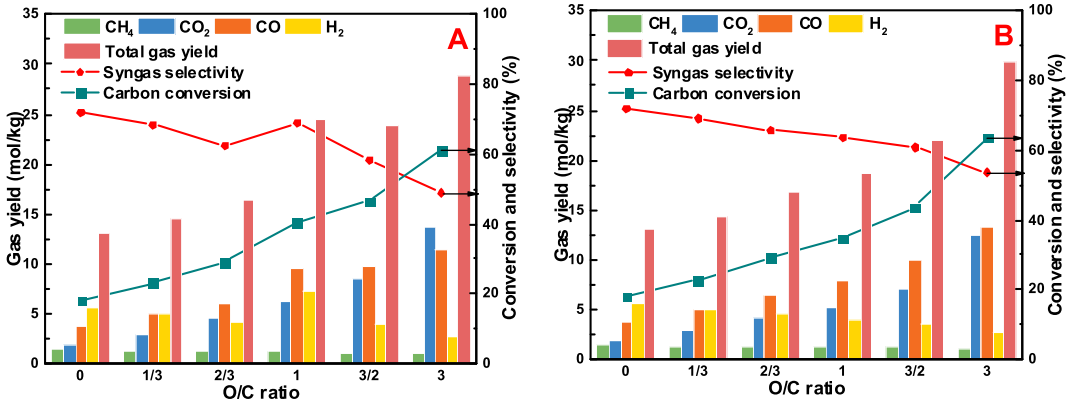

Fig. 8. The effect on oxygen carrier to coal ratio (O/C) on chemical looping gasification of lignite over $NiFe_2O_4$ synthesized by different methods. Blank: pyrolysis of lignite without oxygen carrier. Gasification temperature: 900 °C, Reaction time: 60 min, Ar flowrate: 100 ml/min. A: $NiFe_2O_4$ synthesized by sol–gel method, B: $NiFe_2O_4$ synthesized by solid-phase method.

than its consumption reactions.

The comparison of the performance of four oxygen carriers during chemical looping gasification of lignite under the optimal operating conditions is given in Fig. 9. It is obvious that, among the four oxygen carriers, $NiFe_2O_4$ synthesized by sol–gel method exhibits the highest carbon conversion of 40.4%, the highest total gas yield of 24.47 mol/kg, the highest H_2 yield of 7.32 mol/kg, the highest syngas selectivity of 69.0, and the highest H_2/CO ratio of 0.77. It is thus concluded that the $NiFe_2O_4$ synthesized by so-gel method is the best oxygen carrier for maximizing the production of H_2, which is also corresponded to its best activity of TG results. During the sol–gel synthesis process, nitrate can be mixed more uniformly and highly cubic spinel structure can be obtained to improve the mobility of lattice oxygen and enhance the metal synergistic effect. Besides, the combustion of organic material (citric acid) initially during the calcination process may be beneficial for the porous structure of the sample [39]. Compared to $CuFe_2O_4$, Fe-Ni synergistic effect provided higher gasification reactivity with lignite char which is very important for the coal gasification since char accounting for more than 30% in pyrolysis products. Huang et al. investigated ferrites as oxygen carriers for chemical looping gasification of biomass and found that the presence of Fe-Ni alloy phase and Fe-Ni spinel structure phase facilitated the rupture of C–C bonds and C–H bond [40]. $NiFe_2O_4$ has good oxidizing capacity for solid fuel gasification and its reduced products have good performance for tar cracking. All these reported results are consistent with our experiments. However, its gasification performance, especially the carbon conversion and H_2/CO of syngas, is still unsatisfactory. The addition of steam is a simple and effective method to further improve its gasification performance.

3.5. The H_2-rich syngas production from chemical looping gasification of lignite over $NiFe_2O_4$ in the presence of steam

Steam was added to chemical looping gasification of lignite as an additional gasifying agent to promote the production of hydrogen-rich syngas. The effect of the steam flowrate on the syngas production from chemical looping gasification of lignite is illustrated in Fig. 10A. It is found that the carbon conversion, gas yield, and syngas selectivity are improved by the addition of steam. As the steam flowrate increases from 0 to 0.1 ml/min, the carbon conversion increases noticeably from 40.4 to 67.5%, while the total gas yield and H_2 yield rises drastically from 24.47 and 7.32 to 64.98 and 36.11 mol/kg, respectively. The results could be due to that the addition of steam can accelerate the direct conversion of lignite char with steam via water–gas reaction. However, the addition of steam can also improve the consumption of CO to form

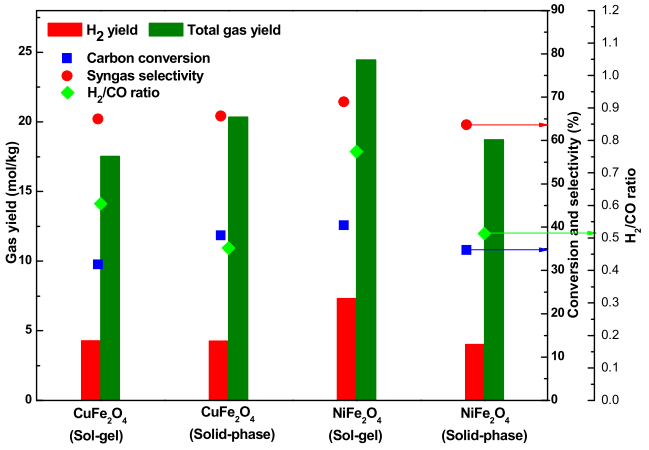

Fig. 9. The comparison of the performance of four oxygen carriers during chemical looping gasification of lignite under the optimal operating conditions. Gasification temperature: 900 °C, O/C ratio = 1, reaction time: 60 min, Ar flowrate: 100 ml/min.

CO_2 and H_2 via water–gas shift reactions. Hence, the syngas selectivity first increases and then decreases as increasing steam flowrate. The maximum syngas selectivity of 77.9% is reached at the steam flowrate of 0.025 ml/min. The effect of steam flowrate on the H_2/CO ratio of syngas from chemical looping gasification of lignite is drawn in Fig. 10B. It is evident that steam can serve as hydrogen source for improving the H_2/CO ratio of syngas via water–gas shift reactions and methane steam reforming reactions. As the steam flowrate increases from 0 to 0.1 ml/min, the H_2/CO ratio rises from 0.77 to 2.79, suggesting that the H_2/CO ratio of syngas can be flexibly adjusted to meet the need of downstream process via controlling the steam flowrate. It is well known that increasing the concentration of steam as reactant shifts the chemical equilibrium of water–gas shift reaction towards the right based on Le Chatelier's principle. The results are in line with the fact that the H_2 and CO_2 yields rise progressively with increasing steam flowrate.

3.6. Surface morphology analysis of fresh, reduced, and regenerated oxygen carriers

The surface morphology of the fresh, reduced, and regenerated $NiFe_2O_4$ oxygen carriers was characterized by SEM. As shown in Fig. 11, the surface of the fresh $NiFe_2O_4$ is smooth and dense, with a few of pore structures existed on its surface. After reaction with lignite, the surface of the reduced $NiFe_2O_4$ is relatively rough and more pore structures and smaller particle sizes are shown, which may be resulted from the transfer of lattice oxygen within $NiFe_2O_4$ to lignite via gasification reactions. After regeneration with air, very regular pore structures are observed on the surface of regenerated $NiFe_2O_4$. These pore structures could be formed by the combustion of char and coke within reduced oxygen carrier. Serious sintering and agglomeration phenomena are not found in the reduced and regenerated oxygen carriers, suggesting the $NiFe_2O_4$ oxygen carrier synthesized by sol–gel method is a good candidate for achieving of efficient gasification of lignite.

4. Conclusion

It is demonstrated that, among four types of oxygen carrier, $NiFe_2O_4$ synthesized by sol–gel method exhibits the highest gasification reactivity with lignite char at an O/C ratio of 1. XRD and H_2-TPR analysis shows that the highly pure cubic spinel structure of this oxygen carrier is beneficial to improve the mobility of lattice oxygen. Furthermore, the operating conditions for chemical looping gasification of lignite were optimized and the gasification performance of four types oxygen carriers was compared by using a fixed bed reactor. The optimal gasification temperature, reaction time, and Ar flowrate for chemical looping gasification of lignite are 900 °C, 60 min, and 100 ml/min, respectively. And the $NiFe_2O_4$ synthesized by sol–gel method exhibits the highest total gas yield of 24.47 mol/kg and H_2/CO ratio of 0.77 during chemical looping gasification of lignite under the optimal operating conditions. However, its gasification performance, especially the carbon conversion and H_2/CO ratio of syngas, is still unsatisfactory. The addition of steam significantly improves its gasification performance. The addition of steam drastically improves the total gas yield and H_2/CO ratio of syngas from 24.47 mol/kg and 0.77 to 64.98 mol/kg and 2.79. Considering the good performance of $NiFe_2O_4$ for solid–solid reaction during coal gasification, combining with the advantages such as the relatively cheap price of raw materials and the easy preparation process that been able to scale up, $NiFe_2O_4$ would be a promising selection for the coal chemical looping technology. These findings provide a novel and efficient method to obtain H_2-rich syngas via chemical looping gasification of lignite.

CRediT authorship contribution statement

Kun Zhao: Data curation, Formal analysis, Writing - original draft. **Xiaojie Fang:** Data curation. **Zhen Huang:** Writing - review & editing. **Guoqiang Wei:** Writing - review & editing. **Anqing Zheng:** Funding

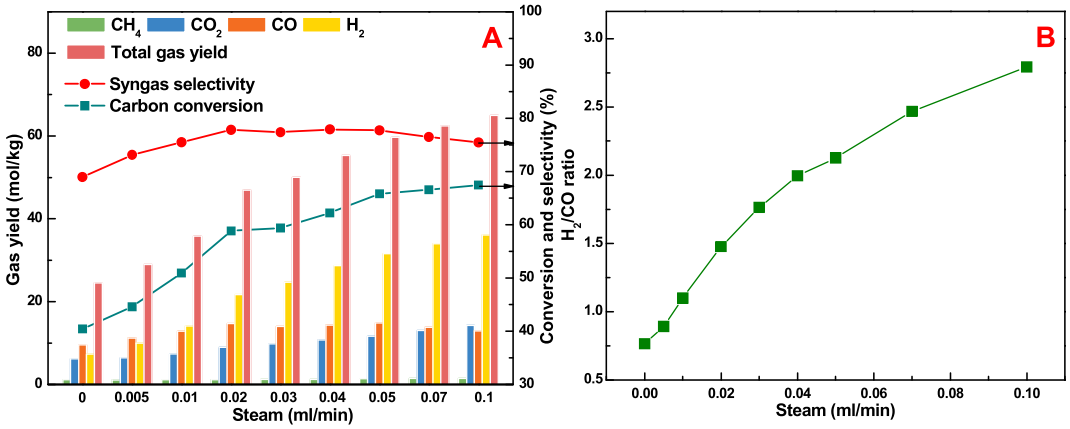

Fig. 10. The effect of steam flowrate on the syngas production from chemical looping gasification of lignite. Oxygen carrier: $NiFe_2O_4$ synthesized by sol–gel method, gasification temperature: 900 °C, O/C ratio = 1, reaction time: 60 min, Ar flowrate: 100 ml/min. A: gas yield, carbon conversion and syngas selectivity, B: H_2/CO ratio of syngas.

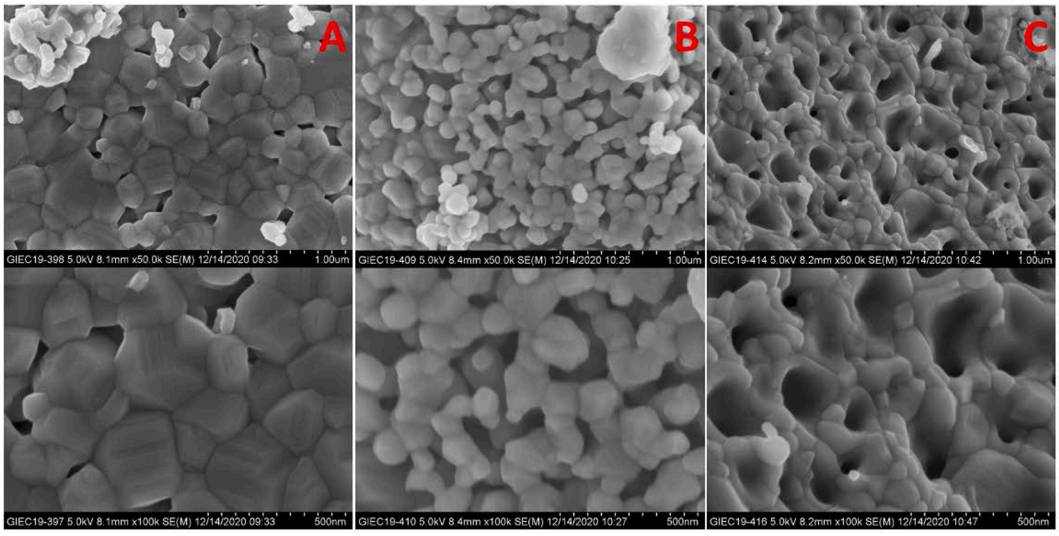

Fig. 11. SEM images of fresh, reduced, and regenerated $NiFe_2O_4$ oxygen carrier synthesized by sol–gel method oxygen carriers. A: fresh $NiFe_2O_4$, B: reduced $NiFe_2O_4$ obtained from chemical looping gasification of lignite at 900 °C with steam, C: regenerated $NiFe_2O_4$.

acquisition, Supervision, Writing - review & editing. **Zengli Zhao:** Supervision.

Declaration of Competing Interest

The authors declare that they have no known competing financial interests or personal relationships that could have appeared to influence the work reported in this paper.

Acknowledgements

The authors gratefully acknowledge the National Key R&D Program of China (Grant 2018YFB0605402), National Natural Science Foundation of China (51876205), Youth Innovation Promotion Association, CAS (2019341, 2018383), and the Pearl River S&T Nova Program of Guangzhou (Grant 201906010092, 201806010061) for their financial support of this work.

References

[1] Plc BP. BP statistical review of world energy 2020. In: BP statistical review of world energy 2020. 69 ed. 2020. p. 1–65.
[2] Rauch R, Hrbek J, Hofbauer H. Biomass gasification for synthesis gas production and applications of the syngas. WIRES Energy Environ 2014;3(4):343–62.
[3] Prins MJ, Ptasinski KJ, Janssen FJJG. More efficient biomass gasification via torrefaction. Energy 2006;31(15):3458–70.
[4] Dhyani V, Bhaskar T. A comprehensive review on the pyrolysis of lignocellulosic biomass. Renew Energ 2018;129:695–716.
[5] Sansaniwal SK, Pal K, Rosen MA, Tyagi SK. Recent advances in the development of biomass gasification technology: A comprehensive review. Renew Sust Energ Rev 2017;72:363–84.
[6] Huang Z, He F, Feng Y, Zhao K, Zheng A, Chang S, et al. Biomass char direct chemical looping gasification using NiO-modified iron ore as an oxygen carrier. Energ Fuel 2014;28(1):183–91.
[7] Guo Q, Cheng Yu, Liu Y, Jia W, Ryu H-J. Coal chemical looping gasification for syngas generation using an iron-based oxygen carrier. Ind Eng Chem Res 2014;53 (1):78–86.
[8] Acharya B, Dutta A, Basu P. Chemical-looping gasification of biomass for hydrogen-enriched gas production with in-process carbon dioxide capture. Energ Fuel 2009;23(10):5077–83.
[9] Zeng J, Xiao R, Zeng D, Zhao Y, Zhang H, Shen D. High H2/CO ratio syngas production from chemical looping gasification of sawdust in a dual fluidized bed gasifier. Energ Fuel 2016;30(3):1764–70.
[10] Wu Y, Liao Y, Liu G, Ma X. Syngas production by chemical looping gasification of biomass with steam and CaO additive. Int J Hydrogen Energ 2018;43(42): 19375–83.
[11] Liu G, Liao Y, Wu Y, Ma X. Synthesis gas production from microalgae gasification in the presence of Fe2O3 oxygen carrier and CaO additive. Appl Energ 2018;212: 955–65.
[12] Tian X, Niu P, Ma Y, Zhao H. Chemical-looping gasification of biomass: Part II. Tar yields and distributions. Biomass Bioenerg 2018;108:178–89.

[13] Hu J, Li C, Guo Q, Dang J, Zhang Q, Lee D-J, et al. Syngas production by chemical-looping gasification of wheat straw with Fe-based oxygen carrier. Bioresource Technol 2018;263:273–9.
[14] Niu P, Ma Y, Tian X, Ma J, Zhao H. Chemical looping gasification of biomass: Part I. screening Cu-Fe metal oxides as oxygen carrier and optimizing experimental conditions. Biomass Bioenerg 2018;108:146–56.
[15] Adánez J, de Diego LF, García-Labiano F, Gayán P, Abad A, Palacios JM. Selection of oxygen carriers for chemical-looping combustion. Energ Fuel 2004;18(2):371–7.
[16] Fan Y, Tippayawong N, Wei G, Huang Z, Zhao K, Jiang L, et al. Minimizing tar formation whilst enhancing syngas production by integrating biomass torrefaction pretreatment with chemical looping gasification. Appl Energ 2020;260:114315. https://doi.org/10.1016/j.apenergy.2019.114315.
[17] Gao N, Li A, Quan C, Gao F. Hydrogen-rich gas production from biomass steam gasification in an updraft fixed-bed gasifier combined with a porous ceramic reformer. Int J Hydrogen Energ 2008;33(20):5430–8.
[18] Li F, Kim HR, Sridhar D, Wang F, Zeng L, Chen J, et al. Syngas chemical looping gasification process: oxygen carrier particle selection and performance. Energ Fuel 2009;23(8):4182–9.
[19] Li D, Xu R, Li X, Li Z, Zhu X, Li K. Chemical looping conversion of gaseous and liquid fuels for chemical production: a review. Energ Fuel 2020;34(5):5381–413.
[20] Adanez J, Abad A, Garcia-Labiano F, Gayan P, de Diego LF. Progress in chemical-looping combustion and reforming technologies. Prog Energ Combust 2012;38(2):215–82.
[21] Zeng J, Xiao R, Zhang S, Zhang H, Zeng D, Qiu Yu, et al. Identifying iron-based oxygen carrier reduction during biomass chemical looping gasification on a thermogravimetric fixed-bed reactor. Appl Energ 2018;229:404–12.
[22] Wei G, wang H, Zhao W, Huang Z, Yi Q, He F, et al. Synthesis gas production from chemical looping gasification of lignite by using hematite as oxygen carrier. Energ Convers Manage 2019;185:774–82.
[23] Shen L, Wu J, Gao Z, Xiao J. Characterization of chemical looping combustion of coal in a 1 kWth reactor with a nickel-based oxygen carrier. Combust Flame 2010;157(5):934–42.
[24] Dennis JS, Scott SA. In situ gasification of a lignite coal and CO2 separation using chemical looping with a Cu-based oxygen carrier. Fuel 2010;89(7):1623–40.
[25] Ge H, Shen L, Feng F, Jiang S. Experiments on biomass gasification using chemical looping with nickel-based oxygen carrier in a 25 kWth reactor. Appl Therm Eng 2015;85:52–60.
[26] Xie Q, Borges FC, Cheng Y, Wan Y, Li Y, Lin X, et al. Fast microwave-assisted catalytic gasification of biomass for syngas production and tar removal. Bioresource Technol 2014;156:291–6.
[27] Li T, Wu Q, Wang W, Xiao YuPeng, Liu C, Yang F. Solid-solid reaction of CuFe2O4 with C in chemical looping system: A comprehensive study. Fuel 2020;267:117163. https://doi.org/10.1016/j.fuel.2020.117163.
[28] Castellanos-Beltran IJ, Perreault L-S, Braidy N. Application of Ni–Spinel in the Chemical-Looping Conversion of CO2 to CO via Induction-Generated Oxygen Vacancies. J Phys Chem C 2021;125(13):7213–26.
[29] He F, Huang Z, Wei G, Zhao K, Wang G, Kong X, et al. Biomass chemical-looping gasification coupled with water/CO2-splitting using NiFe2O4 as an oxygen carrier. Energ Convers Manage 2019;201:112157. https://doi.org/10.1016/j.enconman.2019.112157.
[30] Sturzenegger M, Dsouza L, Struis R, Stucki S. Oxygen transfer and catalytic properties of nickel iron oxides for steam reforming of methane. Fuel 2006;85(10-11):1599–602.
[31] Niu X, Shen L, Jiang S, Gu H, Xiao J. Combustion performance of sewage sludge in chemical looping combustion with bimetallic Cu–Fe oxygen carrier. Chem Eng J 2016;294:185–92.
[32] Zhu X, Zhang J, Yan J, Shen L. Characteristic Evaluation and Process Simulation of CuFe2O4 as Oxygen Carriers in Coal Chemical Looping Gasification. ACS Omega 2021;6(7):4783–92.
[33] Din IU, Tasleem S, Naeem A, Shaharun MS, Nasir Q. Study of annealing conditions on particle size of nickel ferrite nanoparticles synthesized by wet chemical route. Synth React Inorg, Met-Org, Nano-Met Chem 2016;46(3):405–8.
[34] Xiong Mi, Gao Z, Qin Y. Spillover in Heterogeneous Catalysis: New Insights and Opportunities. ACS Catal 2021;11(5):3159–72.
[35] Yan J, Bai Z, Bai J, Guo Z, Li W. Effects of organic solvent treatment on the chemical structure and pyrolysis reactivity of brown coal. Fuel 2014;128:39–45.
[36] Tian X, Su M, Zhao H. Kinetics of redox reactions of CuO@ TiO2–Al2O3 for chemical looping combustion and chemical looping with oxygen uncoupling. Combust Flame 2020;213:255–67.
[37] Hu Z, Jiang E, Ma X. The effect of oxygen carrier content and temperature on chemical looping gasification of microalgae for syngas production. J Energy Inst 2019;92(3):474–87.
[38] Chen L, Bao J, Kong L, Combs M, Nikolic HS, Fan Z, et al. The direct solid-solid reaction between coal char and iron-based oxygen carrier and its contribution to solid-fueled chemical looping combustion. Appl Energ 2016;184:9–18.
[39] Liu S, He F, Huang Z, Zheng A, Feng Y, Shen Y, et al. Screening of NiFe2O4 nanoparticles as oxygen carrier in chemical looping hydrogen production. Energ Fuel 2016;30(5):4251–62.
[40] Huang Z, Deng Z, Chen D, He F, Liu S, Zhao K, et al. Thermodynamic analysis and kinetic investigations on biomass char chemical looping gasification using Fe-Ni bimetallic oxygen carrier. Energy 2017;141:1836–44.